Michiels Laura (Orcid ID: 0000-0002-1208-5334)
Mertens Nathalie (Orcid ID: 0000-0002-2409-7586)
Coremans Marjan (Orcid ID: 0000-0002-4331-892X)

Longitudinal synaptic density PET with ^{11}C-UCB-J 6 months after ischemic stroke

Laura Michiels, MD PhD[1,2,3,4]; Liselot Thijs, PhD[5]; Nathalie Mertens, PhD[6]; Marjan Coremans, MSc[5]; Mathieu Vandenbulcke, MD PhD[1,4,7]; Geert Verheyden, PhD[5]; Michel Koole, PhD[6]; Koen Van Laere, MD PhD[4,6,7]; Robin Lemmens, MD PhD[1,2,3,4]

1. Department of Neurosciences, KU Leuven, Belgium
2. VIB, Center for Brain & Disease Research, Laboratory of Neurobiology, Belgium
3. Department of Neurology, University Hospitals Leuven, Belgium
4. Leuven Brain Institute, KU Leuven, Belgium
5. Department of Rehabilitation Sciences, KU Leuven, Belgium
6. Nuclear Medicine and Molecular Imaging, Department of Imaging and Pathology, KU Leuven, Belgium
7. Department of Geriatric Psychiatry, University Psychiatric Centre, KU Leuven, Belgium
8. Department of Nuclear Medicine, University Hospitals Leuven, Belgium

Corresponding author

Laura Michiels (ORCID-ID: 0000-0002-1208-5334), MD, resident in Neurology

laura.michiels@uzleuven.be – Tel:003216345508 – Fax:003216343759

Department of Neurology, University Hospitals Leuven, Herestraat 49, 3000 Leuven, Belgium

Running head: SV2A PET 6 months after ischemic stroke

Character count: Title: 79; running head: 39

Word count: Abstract: 244; Introduction: 460; Discussion: 1565; Total body of the manuscript: 3857

Number of references: 40

Number of tables: 3

Number of figures: 5

Number of color figures: 3

This article has been accepted for publication and undergone full peer review but has not been through the copyediting, typesetting, pagination and proofreading process which may lead to differences between this version and the Version of Record. Please cite this article as doi: 10.1002/ana.26593

SUMMARY FOR SOCIAL MEDIA IF PUBLISHED

What is the current knowledge on the topic?

Neural plasticity is a key factor driving recovery after stroke and certain brain regions have been associated with motor recovery post stroke.

What question did this study address?

Can we visualize neural plasticity after stroke by synaptic density PET imaging? Do changes occur in the brain regions previously associated with motor recovery?

What does this study add to our knowledge?

This study demonstrates that synaptic density, as measured with SV2A PET, further declines over 6 months after stroke. None of the brain regions previously associated with motor recovery shows an increase in synaptic density.

How might this potentially impact on the practice of neurology?

Unravelling the mechanisms underlying functional recovery after stroke may aid in optimizing rehabilitation and development of pro-restorative therapies.

ABSTRACT

Objective

To explore longitudinal changes in synaptic density after ischemic stroke in vivo with synaptic vesicle protein 2A (SV2A) PET.

Methods

We recruited patients with an ischemic stroke to undergo ^{11}C-UCB-J PET/MR within the first month and 6 months after stroke. We investigated longitudinal changes of partial volume corrected ^{11}C-UCB-J SUVR (standardized uptake value ratio; relative to centrum semiovale) within the ischemic lesion, peri-ischemic area and unaffected ipsilesional and contralesional grey matter. We also explored crossed cerebellar diaschisis at 6 months. Additionally, we defined brain regions potentially influencing upper limb motor recovery after stroke and studied ^{11}C-UCB-J SUVR evolution in comparison to baseline.

Results

In 13 patients (age = 67±15 years) we observed decreasing ^{11}C-UCB-J SUVR in the ischemic lesion (ΔSUVR = -1.0, p=0.001) and peri-ischemic area (ΔSUVR = -0.31, p=0.02) at 6 months after stroke compared to baseline. Crossed cerebellar diaschisis as measured with ^{11}C-UCB-J SUVR was present in 11/13 (85%) patients at 6 months. ^{11}C-UCB-J SUVR did not augment in ipsilesional or contralesional brain regions associated with motor recovery. On the contrary, there was an overall trend of declining ^{11}C-UCB-J SUVR in these brain regions, reaching statistical significance only in the non-lesioned part of the ipsilesional supplementary motor area (ΔSUVR = -0.83, p=0.046).

Interpretation

At 6 months after stroke, synaptic density further declined in the ischemic lesion and peri-ischemic area compared to baseline. Brain regions previously demonstrated to be associated with motor recovery after stroke did not show increases in synaptic density.

INTRODUCTION

Recovery after stroke in human is a complex phenomenon of which the biological basis remains incompletely understood. Neural plasticity, which includes reorganization of networks driven by axonal sprouting as well as reinforcement of existing, redundant connections, has been suggested to drive motor recovery.[1–4] Functional neuroimaging studies aimed to visualize reorganization of the motor system of the brain after stroke using functional magnetic resonance imaging (fMRI) or positron emission tomography (PET).[5,6] Both techniques determined relative cerebral blood flow as measure of functional (over)activation during active or passive motor tasks to potentially provide insights in the spatial reorganization patterns underlying functional motor recovery after stroke. Motor regions as well as non-motor regions in both hemispheres became (over)activated during upper limb motor tasks. In general, ipsilesional activation was associated with improved motor recovery and an opposite relationship was present for contralesional activation. This suggests patterns of ipsilesional activation, which represent the normal balance between the two hemispheres, to be more favorable in response to injury.[5,6]

In the past years, novel PET tracers targeting synaptic vesicle protein 2A (SV2A), a protein ubiquitously expressed in all presynaptic nerve terminals, have been developed. SV2A PET tracer binding is seen as proxy for synaptic density.[7–9] Importantly, although in general PET is considered a functional imaging modality, SV2A PET rather reflects a structural correlate of synaptic function. In contrast to perfusion PET and fMRI, in which performance of a task relates to changes in PET/fMRI signal in task-related brain regions, SV2A PET signal is independent of brain region activation.[10] Performing motor tasks during acquisition of SV2A PET is redundant, simplifying the study design compared to previous neuroimaging studies investigating motor recovery after stroke. SV2A PET may be an interesting imaging modality to study neural plasticity after stroke in vivo as it might be able to measure the underlying structural correlate of reorganization. We have previously demonstrated the feasibility of SV2A PET in subacute ischemic stroke patients where we showed a decrease of synaptic density within the ischemic lesion and the ipsilesional cerebral hemisphere within the first month after stroke.

Moreover, crossed cerebellar diaschisis could be detected with SV2A PET in 50% of patients, reflecting disruption of cerebro-cerebellar pathways.[11]

In the present longitudinal follow-up study, we assessed the temporal dynamics of changes in synaptic density 6 months after ischemic stroke within the ischemic lesion and peri-ischemic area as well as in the unaffected ipsilesional and contralesional grey matter. We also explored the evolution in crossed cerebellar diaschisis. Additionally, based on functional neuroimaging studies, we delineated a priori defined brain regions in which previously activation was demonstrated in relation to upper limb motor tasks and we studied potential increases in synaptic density in these areas.[5] Finally, we tested correlations between SV2A tracer binding and upper limb motor function.

METHODS

This study was approved by the local University Hospital Research Ethics Committee (UZ Leuven / KU Leuven) and was conducted in accordance with the latest version of the Declaration of Helsinki. All participants (or relatives in case the patient was unable to give written informed consent) signed written informed consent prior to participation. This study is part of a larger multimodal, multitracer longitudinal imaging study (ClinicalTrials.gov: NCT03514524). The results of the baseline SV2A data of this cohort of stroke patients have been published previously.[11] The data that support the findings of this study are not publicly available due to privacy/ethical restrictions. Upon reasonable request, the anonymized data could be shared on approval by the local Ethics Committee.

Participants and study design

Detailed in- and exclusion criteria of patients can be found in the baseline paper.[11] In short, we recruited patients between 18-85 years with a first ischemic supratentorial stroke and a substantial motor deficit of the upper limb (defined as Medical Research Council [MRC] grade 3 or less for finger extension and/or elbow flexion and/or shoulder abduction) to undergo ^{11}C-UCB-J PET/MR (magnetic resonance) within the first 2 to 4 weeks after stroke as well as 6 months after the index event. In addition to neuroimaging studies, patients also underwent a clinical test battery at inclusion (National Institutes of Health Stroke Scale [NIHSS], Barthel Index [BI], Fugl-Meyer Upper Extremity [FMUE] and Lower Extremity [FMLE] and Functional Ambulation Categories [FAC]) and at 6 months follow up (BI, FMUE, FMLE, FAC and Action Research Arm Test [ARAT]).

Image acquisition and reconstruction

All participants underwent 30 minutes simultaneous ^{11}C-UCB-J PET/MR imaging starting 60 minutes post tracer injection on a General Electric (GE, Milwaukee, WI, USA) Signa PET/MR (time-of-flight [TOF] PET, 3 Tesla MR) at two time points. Median injected ^{11}C-UCB-J activity was 215 MBq (IQR: 209-230 MBq) at baseline and 198 MBq (IQR: 174-211 MBq) at follow up with mean specific activity of 227±135 GBq/µmol and 217±79 GBq/µmol respectively. PET acquisitions were performed in list mode, rebinned

into 6 frames of 5 minutes and reconstructed using vendor software. As reconstruction algorithm, an ordered subset expectation maximization (28 subsets, 4 iterations) was used including TOF information and decay, scatter, attenuation, deadtime and random correction. Isotropic Gaussian post smoothing was performed to reduce the noise (full width at half maximum [FWHM] of 4 mm; final image resolution 5 mm). Individual attenuation correction was performed using a validated zero echo time (ZTE) approach.[12] We acquired 3D T1-weighted as well as 3D T2-weighted FLAIR images at both time points.

Image processing

At baseline, we defined the stroke lesions semi-automatically using 3D T2-weighted FLAIR data. For lesion delineation at 6 months follow up, we co-registered the MR data and lesion mask from baseline imaging to the MR data at follow up and adapted the lesion mask according to the T2-weighted FLAIR data at 6 months follow up. Subsequently, we created a peri-ischemic area by applying a 4 mm simple binary dilation of the lesion mask at both time points. We adapted the peri-ischemic areas manually to exclude voxels not consisting of brain parenchyma. Figure 1 shows an example of a delineated ischemic lesion and peri-ischemic area. In addition to the ischemic lesion and peri-ischemic area, we defined the unaffected ipsilesional and contralesional grey matter as all cerebral grey matter not belonging to the lesion or peri-ischemic area (Figure 1) and we were interested in the cerebellum to evaluate crossed cerebellar diaschisis. Furthermore, we selected ipsi- and contralesional brain regions potentially modifying upper limb motor recovery, based on literature: primary sensorimotor cortex, supplementary motor area, premotor cortex, prefrontal cortex, cingulate cortex, parietal cortex, insula, striatum and cerebellum.[5] As the large cortical stroke lesions could interfere with proper automated delineation of volumes-of-interest (VOI), we preprocessed the T1-weighted MR data of patients with cortical lesion involvement using virtual brain grafting (version 4).[13] In this pipeline the manually delineated cortical lesion is replaced by healthy tissue based on the contralesional hemisphere. These *healthy* T1-weighted images are then used as input for VOI delineation in

FreeSurfer (Laboratory for Computational Neuroimaging v6.0, Boston, USA; cortical parcellation based on the Desikan-Killiany atlas,[14,15] subcortical structures as described in Fischl *et al.*[16]) and VOI delineation based on the Human Motor Area Template (HMAT;[17] see Supplementary Table 1 for exact VOI definitions).

We preprocessed ^{11}C-UCB-J PET images using PMODv3.9 (PMOD technologies, Zurich, Switzerland): first, motion correction was applied by rigidly realigning each frame to the first frame, then averaging all frames. Second, we co-registered the PET images to the corresponding T1-weighted MR data and calculated standardized uptake value ratios (SUVR) using the contralesional centrum semiovale as reference region (see [11] for detailed description).[18–21] Representative ^{11}C-UCB-J SUVR images and their corresponding T2 FLAIR images of 3 patients are shown in Figure 2. We applied a region-based voxel-wise (RBV) partial volume correction technique on the SUVR images to account for partial volume effects (point spread function of 5 mm). Hereby, we used the VOIs as delineated with FreeSurfer and merged small VOIs into larger composite VOIs to prevent calculations with numerous small regions resulting in less robust RBV estimation. Moreover, the parts of the VOIs that belonged to the lesion were considered as separate VOIs as we expected the uptake to be heterogeneous if lesion boundaries were crossed. We extracted a volume-weighted average ^{11}C-UCB-J SUVR value (with partial volume correction) for each VOI. For clarity, these values represent the average ^{11}C-UCB-J SUVR of the total VOI, irrespective of stroke lesion involvement. However, as the decrease of ^{11}C-UCB-J SUVR in the lesion (see Results) could influence the results of the ipsilesional brain regions potentially modifying upper limb motor recovery, we also analyzed these VOIs taking a volume-weighted average ^{11}C-UCB-J SUVR value of only the non-lesioned voxels.

Statistics

We performed general statistics in RStudio (v1.1.463. RStudio, Inc., Boston, MA) and we presented the data as mean ± standard deviation if normally distributed and as median (interquartile range [IQR]) if not normally distributed. We verified normality of distributions with Shapiro-Wilk tests (α = 0.05).

To investigate longitudinal evolution of ^{11}C-UCB-J SUVR in the lesion, peri-ischemic area and unaffected ipsilesional and contralesional grey matter, we performed paired t-tests. To investigate the correlation between lesion volume and ^{11}C-UCB-J SUVR, we used Spearman correlation.

To evaluate crossed cerebellar diaschisis, we calculated individual cerebellar asymmetry indices (AI's):[22–24]

$$AI = \frac{SUVR_{ipsilesional\ cerebellum} - SUVR_{contralesional\ cerebellum}}{SUVR_{ipsilesional\ cerebellum}} * 100$$

AI's of patients were considered significantly asymmetric if they exceeded the mean ± 2 standard deviation boundaries (= z-score >2 of <-2) of the AI's of controls. We used our previously published ^{11}C-UCB-J AI's of 40 controls to derive cut-off values.[11] A significant AI in disfavor of the contralesional cerebellar hemisphere (= positive AI value) is the hallmark of crossed cerebellar diaschisis. We also analyzed the longitudinal evolution of AI in patients with a paired t-test.

To assess ^{11}C-UCB-J SUVR in the VOIs that could potentially modify upper limb motor recovery, we performed paired t-tests or Wilcoxon signed rank tests as appropriate.

To investigate the correlation between ^{11}C-UCB-J SUVR and upper limb motor outcome at 6 months (FMUE, ARAT), we used Pearson or Spearman correlation as appropriate. To investigate the correlation between ^{11}C-UCB-J SUVR and upper limb motor recovery (ΔFMUE), we calculated ΔSUVR and $\Delta FMUE_{relative}$ and correlated them using Pearson or Spearman correlation as appropriate.

$$\Delta SUVR_{absolute} = SUVR_{follow\ up} - SUVR_{baseline}$$

$$\Delta SUVR_{relative} = \frac{SUVR_{follow\ up} - SUVR_{baseline}}{SUVR_{baseline}}$$

$$\Delta FMUE_{relative} = \frac{FMUE_{follow\ up} - FMUE_{baseline}}{66 - FMUE_{baseline}}$$

with 66 being the maximum score for FMUE.

As this study was exploratory, significance level for all statistical analyses was set to $\alpha = 0.05$ without correction for multiple testing.

RESULTS

Patient characteristics

We included 23 patients with a first ischemic stroke of whom 21 underwent baseline ^{11}C-UCB-J PET/MR imaging. Of these 21 patients, 13 patient underwent follow up ^{11}C-UCB-J PET/MR imaging at 6 months after stroke. Only patients with baseline and follow up imaging were included in the analyses. Table 1 describes the demographic, clinical and neuroimaging characteristics of these 13 patients. A lesion overlap image of the baseline lesions of all included patients is shown in Figure 3. Changes in FMUE over time are visualized in Figure 4.

Changes in ^{11}C-UCB-J SUVR within the ischemic lesion and peri-ischemic area

Mean ^{11}C-UCB-J SUVR in the ischemic lesion was 1.57±0.93 at baseline (lower compared to controls)[11] and further decreased to 0.57±0.26 at 6 months follow up (p=0.001). The earlier reported decline in ^{11}C-UCB-J SUVR in the peri-ischemic area also advanced over time (2.88±0.53 vs. 2.57±0.41, p=0.02). There was no correlation between lesion volume and ^{11}C-UCB-J SUVR within the lesion (r_S = 0.13, p=0.68) at 6 months after stroke.

Changes in ^{11}C-UCB-J SUVR in unaffected ipsilesional and contralesional grey matter

There was no decline in ^{11}C-UCB-J SUVR over time in the unaffected ipsilesional grey matter (7.22±1.02 vs. 6.85±0.95, p=0.22), nor in the contralesional grey matter (7.49±0.96 vs. 7.03±0.92, p=0.46). At 6 months after stroke, ^{11}C-UCB-J SUVR in the unaffected ipsilesional grey matter negatively correlated with lesion volume (r_S = -0.77, p=0.003), but this correlation was not identified in the contralesional grey matter (r_S = -0.54, p=0.06).

Crossed cerebellar diaschisis measured with ^{11}C-UCB-J PET at 6 months after stroke

As shown in Table 2, ^{11}C-UCB-J SUVR in the contralesional cerebellum declined over time in stroke patients. Cerebellar AI's are visualized in Figure 5. The cerebellar AI was consistent with crossed cerebellar diaschisis in 11 patients (85%) at 6 months follow up compared to 9 patients (69%) at

baseline. When evaluating the cerebellar AI longitudinally, the asymmetries trended to rise over time (baseline: 5.2±4.6, follow up: 8.1±5.2, p=0.06).

Changes in ^{11}C-UCB-J SUVR in brain regions potentially modifying upper limb motor recovery

Longitudinal results of ^{11}C-UCB-J SUVR in brain regions that potentially modify upper limb motor recovery are shown in Table 2. At 6 months follow up, there was a reduction of ^{11}C-UCB-J SUVR in the ipsilesional supplementary motor area, premotor cortex and prefrontal cortex (as well as in the contralesional cerebellum, see above) compared to baseline. As some of these brain regions consisted, at least partially, of the ischemic lesion itself, we also calculated these ipsilesional VOIs after excluding voxels that belonged to the ischemic lesion. In this analysis, most regions trended towards a decline of ^{11}C-UCB-J SUVR over time, but only the ipsilesional supplementary motor area reached statistical significance (see Table 3).

Correlation between ^{11}C-UCB-J SUVR and upper limb motor function

When testing the correlation between ^{11}C-UCB-J SUVR in brain regions potentially modifying upper limb motor recovery and upper limb outcome at 6 months, we found a positive correlation between ^{11}C-UCB-J SUVR in the ipsilesional striatum and FMUE (r_S = 0.75, p=0.003) as well as between ^{11}C-UCB-J SUVR in the ipsilesional striatum and ARAT (r_S = 0.74, p=0.004). However, when calculating these correlations after excluding lesioned voxels, these results were no longer retained. The percentage of lesioned voxels in the ipsilesional striatum negatively correlated with FMUE (r_S = -0.73; p=0.005) and ARAT (r_S = -0.72; p=0.005).

When evaluating the correlation between $\Delta SUVR_{absolute}$ or $\Delta SUVR_{relative}$ and $\Delta FMUE_{relative}$ in all these brain regions after excluding lesioned voxels, we found no correlation in any of the VOIs.

DISCUSSION

In this longitudinal ^{11}C-UCB-J PET/MR study in ischemic stroke patients we were able to determine a further decline in synaptic density over time in the ischemic lesion and peri-ischemic area. The previously reported crossed cerebellar diaschisis persisted at 6 months after stroke. We could not detect increases in synaptic density at 6 months after stroke in any of the selected brain regions associated with upper limb motor recovery, but rather documented a trend towards decline of synaptic density in these brain regions with a significant decrease in the ipsilesional supplementary motor area only.

The longitudinal decline of synaptic density within the ischemic lesion likely reflects progressive tissue loss. In the peri-ischemic area we observed a similar progressive reduction over the months of follow up probably as a consequence of anterograde (Wallerian) and retrograde (Wallerian-like) degeneration. A previous ^{18}F-flumazenil PET study also found that interhemispheric differences in neuronal density in the peri-infarct cortex increased at 6 months follow up compared to 2 weeks after stroke.[25] In contrast to SV2A PET, which is a presynaptic marker, ^{18}F-flumazenil binds to postsynaptic $GABA_A$ (gamma-aminobutyric acid) receptors, implying that these losses would reflect trans-synaptic degeneration instead of Wallerian(-like) degeneration. For the unaffected ipsilesional and contralesional grey matter we could not determine a significant reduction in synaptic density in the overall cohort. However, the infarct size negatively correlated with synaptic density in the unaffected grey matter of the ipsilesional hemisphere suggestive of remote effects due to loss of connectivity in patients with larger infarcts.

In our baseline study, we described crossed cerebellar diaschisis several weeks after the ischemic injury. Here we show persistence of this diaschisis over months in accordance with studies reporting on this phenomenon several months after the insult.[22,26] However, this contrasts with other studies suggesting diaschisis to be a transient phenomenon as a reflection of temporary functional alterations.[27,28] Differences in included patients, study design and functional imaging modalities utilized to study crossed cerebellar diaschisis could possibly explain this heterogeneity in study results.

However, as SV2A PET can be regarded as structural correlate of synaptic function, our findings may suggest the functional disturbances to be accompanied (or partially explained) by structural alterations. This would imply corticospinal tract damage to lead to trans-synaptic degeneration of ponto-cerebellar pathways. Future neuroimaging studies combining SV2A PET with FDG (fluorodeoxyglucose) PET or perfusion imaging could help distinguish between the contribution of functional versus structural changes.

We analyzed selected brain regions associated with recovery of arm function and identified reduced SV2A PET signal in the ipsilesional supplementary motor area, premotor and prefrontal cortex. The decreases in synaptic density were partially driven by synaptic loss in the ischemic lesion, as we did not observe changes when analyzing the premotor and prefrontal cortex after excluding lesioned voxels. However, even when analyzing only the non-ischemic voxels, there was a trend towards declining synaptic density in most of these regions (reaching statistical significance only in the ipsilesional supplementary motor area). Depending on the localization of the lesion, this decline may represent anterograde (Wallerian) or retrograde (Wallerian-like) degeneration or even trans-synaptic degeneration.

Degeneration of white matter tracts leads to disappearance of presynaptic nerve terminals potentially reflected in reduced SV2A PET signal in the grey matter. Based on the observed decline in synaptic density in the ipsilesional supplementary motor area, peri-ischemic area and contralesional cerebellum, we cautiously postulate SV2A PET as surrogate marker for different forms of degeneration. Future studies comparing diffusion tensor imaging with SV2A PET could aid in assessing the potential of SV2A PET to detect Wallerian, Wallerian-like and trans-synaptic degeneration.

We observed a correlation between ^{11}C-UCB-J SUVR in the ipsilesional striatum at 6 months after stroke and upper limb motor outcome at 6 months. However, this correlation was most likely driven by lesion involvement of the ipsilesional striatum as the correlation was not significant when lesioned voxels were excluded. This was underscored by determining a similar correlation between the proportion of ischemic tissue in the ipsilesional striatum and motor outcome versus the correlation

between ^{11}C-UCB-J SUVR and motor outcome. This suggests the extent to which the ipsilesional striatum is lesioned to relate to upper limb motor outcome and the accompanying decreases in ^{11}C-UCB-J SUVR to reflect tissue loss in the ipsilesional striatum.

Although both cortical and subcortical strokes have been included in previous neuroimaging studies evaluating prognostic markers for recovery, most were restricted to patients with subcortical stroke. Therefore, less is known about motor reorganization after cortical/corticosubcortical stroke.[5,6] It is plausible but currently undetermined if different brain areas are involved in motor recovery following cortical versus subcortical stroke. The importance of the peri-infarct area is thus far mainly reported on after cortical stroke.[3,29–31] We included patients based on severity of upper limb dysfunction instead of lesion pattern and the majority of the patients in our study had cortical lesion involvement. In a critical reflection of the design, one could argue to preferably select patients based on lesion pattern instead of clinical impairment to obtain a more homogenous patient population. However, the rationale for this first study evaluating synaptic plasticity after stroke in humans was to not limit inclusion criteria to one particular stroke pattern in order to explore synaptic reorganization in stroke in general. The small sample size unfortunately hampered the performance of subanalyses based on lesion location.

The lack of elucidating increases in ^{11}C-UCB-J binding in our study may not be misinterpreted as evidence of absence of neural plasticity after ischemic stroke. Study design related factors as small sample size and previously mentioned heterogeneity in included patients may account for this neutral finding. In addition, mean regional test-retest variabilities of ^{11}C-UCB-J PET up to 10%[18,32] may hamper identification of small differences, especially since changes in synaptic density may spatially vary between patients. Moreover, SV2A PET serves as proxy for synaptic density so if the loss of synapses due to the ischemic insult is thereafter compensated (and equaled) by the formation of new synapses, total synaptic density could remain unchanged. However, if axonal sprouting would be a key factor driving neural plasticity, one could expect a net increase in (potentially regional) synaptic density. Importantly, SV2A PET measures density of presynaptic SV2A proteins, proteins that are present in all

presynaptic vesicles,[33] irrespective of the functional pool they belong to. Most synapses rely on three different vesicle pools: the readily releasable pool, the recycling pool and the reserve pool. About 80-90% of vesicles are part of the reserve pool and may never be recruited during physiological activity.[34,35] It is possible that these reserve pool vesicles may play a role in neural plasticity by reinforcement of existing, redundant connections.[36,37] If this strengthening of existing connections by recruitment of reserve pool vesicles is the main component driving neural plasticity, SV2A PET will not be able to visualize neural plasticity as recruitment of pre-existing reserve pool vesicles will not alter SV2A PET measurements.

To further address the ability of SV2A PET to visualize neural plasticity in vivo, it might be useful to investigate conditions with a more homogeneous nature in comparison to stroke (e.g. neural plasticity after motor skill learning or neural plasticity following electroconvulsive therapy as treatment for late-life depression).[38] Future stroke studies might benefit from more homogeneous inclusion criteria (e.g. based on lesion localization or certain FMUE cut-offs) and stratification of patients based on degree of motor recovery. One could aim to compare patients who show proportional recovery versus those who do not in order to determine if differences in synaptic plasticity could partially explain these different trajectories. The sample size in our study was too small to adequately address this question, but comparing synaptic alterations in recoverers versus non-recoverers in a larger cohort would be an interesting approach. We would also recommend switching to fluorine-18 labeled SV2A tracers[8,39,40] which may overcome some of the practical concerns inherent to the short half-life of carbon-11 labeled tracers.

Apart from the small sample size and heterogeneity of patients, the main limitation of our study is the lack of dynamic image acquisition, but this was considered unfeasible in this patient population, especially in the subacute phase and multitracer design. Consequently, we used a previously validated reference tissue normalization quantification method with 60-90 minutes SUVR data normalized on the centrum semiovale. The centrum semiovale is a validated reference tissue for ^{11}C-UCB-J PET imaging in healthy subjects,[18–21] but potential influence of white matter disease on the reference tissue

may be a concern in stroke patients.[11] In the absence of another validated brain region as reference for ^{11}C-UCB-J PET and assuming no significant white matter alterations in the contralesional centrum semiovale to occur over the 6 months follow up, we considered normalization on the centrum semiovale the best available approach. Moreover, there was no difference in SUV of the centrum semiovale between both time points (data not shown). SUVR quantification does not take into account changes in tracer delivery either, but as elaborated on with a simulation in previous study, the bias in SUVR due to changes in tracer delivery is limited (-4.3% - 2.5% for cerebral cortex and -7.2% - 0.0% for cerebellum).[11]

In conclusion, in this SV2A PET study performed within 1 month and at 6 months after ischemic stroke, we identified a longitudinal decrease in synaptic density in the ischemic lesion and peri-ischemic area and we demonstrated crossed cerebellar diaschisis to persist 6 months after stroke. We could not detect increases in ^{11}C-UCB-J SUVR or associations with motor outcome after 6 months.

ACKNOWLEDGEMENTS

This study was supported by an FWO grant (FWO/G093218N) and KU Leuven internal C2 funding (C24-17-063). LT is supported by the grants EU Eurostars project funding, Promobilia and internal KU Leuven funding (internal EU Horizon 2020 runner-up funding). NM is a predoctoral fellow of FWO (= Research Foundation Flanders). KVL and RL are Senior Clinical Investigators of FWO. The authors are grateful to Kwinten Porters and Jef Van Loock for their contribution to the scanning and data handling and the PET radiopharmacy team, the MR radiology team and nuclear medicine medical physics team of UZ Leuven for their skilled contributions.

AUTHOR CONTRIBUTIONS

LM, NM, MV, GV, MK, KVL and RL contributed to the conception and design of the study; LM, LT, NM, MC, GV, MK, KVL and RL contributed to the acquisition and analysis of data; LM and RL contributed to drafting the text or preparing the figures.

POTENTIAL CONFLICTS OF INTEREST

Nothing to report.

DATA AVAILIBILITY

The data that support the findings of this study are not publicly available due to privacy/ethical restrictions. Upon reasonable request, the anonymized data could be shared on approval by the local Ethics Committee.

REFERENCES

1. Pekna M, Pekny M, Nilsson M. Modulation of Neural Plasticity as a Basis for Stroke Rehabilitation. Stroke 2012;43:2819–2828.

2. Sharma N, Cohen LG. Recovery of motor function after stroke. Dev. Psychobiol. 2012;54(3):254–262.

3. Alia C, Spalletti C, Lai S, et al. Neuroplastic Changes Following Brain Ischemia and their Contribution to Stroke Recovery: Novel Approaches in Neurorehabilitation. Front. Cell. Neurosci. 2017;11:76.

4. Murphy TH, Corbett D. Plasticity during stroke recovery: from synapse to behaviour. Nat. Rev. Neurosci. 2009;10(12):861–872.

5. Calautti C, Baron JC. Functional Neuroimaging Studies of Motor Recovery After Stroke in Adults: A Review. Stroke 2003;34:1553–1566.

6. Havsteen I, Madsen KH, Christensen H, et al. Diagnostic approach to functional recovery: functional magnetic resonance imaging after stroke. Front. Neurol. Neurosci. 2013;32:9–25.

7. Nabulsi NB, Mercier J, Holden D, et al. Synthesis and Preclinical Evaluation of 11C-UCB-J as a PET Tracer for Imaging the Synaptic Vesicle Glycoprotein 2A in the Brain. J. Nucl. Med. 2016;57:777–784.

8. Naganawa M, Li S, Nabulsi N, et al. First-in-human evaluation of 18F-SynVesT-1, a radioligand for PET imaging of synaptic vesicle glycoprotein 2a. J. Nucl. Med. 2021;62(4):561–567.

9. Finnema SJ, Nabulsi NB, Eid T, et al. Imaging synaptic density in the living human brain. Sci. Transl. Med. 2016;8(348):348ra96.

10. Smart K, Liu H, Matuskey D, et al. Binding of the synaptic vesicle radiotracer [11C]UCB-J is unchanged during functional brain activation using a visual stimulation task. J. Cereb. Blood Flow Metab. 2021;41(5):1067–1079.

11. Michiels L, Mertens N, Thijs L, et al. Changes in synaptic density in the subacute phase after ischemic stroke: A 11C-UCB-J PET/MR study. J. Cereb. Blood Flow Metab. 2022;42(2):303–314.

12. Schramm G, Koole M, Willekens SMA, et al. Regional accuracy of ZTE-based attenuation correction in static and dynamic brain PET/MR. Front. Phys. 2019;7:211.

13. Radwan AM, Emsell L, Blommaert J, et al. Virtual brain grafting: Enabling whole brain parcellation in the presence of large lesions. Neuroimage 2021;229:117731.

14. Fischl B, van der Kouwe A, Destrieux C, et al. Automatically Parcellating the Human Cerebral Cortex. Cortex 2004;14:11–22.

15. Desikan RS, Ségonne F, Fischl B, et al. An automated labeling system for subdividing the human cerebral cortex on MRI scans into gyral based regions of interest. Neuron 2006;33:341–355.

16. Fischl B, Salat DH, Busa E, et al. Whole Brain Segmentation: Automated Labeling of Neuroanatomical Structures in the Human Brain. Neuron 2002;33:341–355.

17. Mayka MA, Corcos DM, Leurgans SE, Vaillancourt DE. Three-dimensional locations and boundaries of motor and premotor cortices as defined by functional brain imaging: A meta-

analysis. Neuroimage 2006;31(4):1453–1474.

18. Finnema SJ, Nabulsi NB, Mercier J, et al. Kinetic evaluation and test–retest reproducibility of [11C]UCB-J, a novel radioligand for positron emission tomography imaging of synaptic vesicle glycoprotein 2A in humans. J. Cereb. Blood Flow Metab. 2018;38(11):2041–2052.

19. Koole M, van Aalst J, Devrome M, et al. Quantifying SV2A density and drug occupancy in the human brain using [11C]UCB-J PET imaging and subcortical white matter as reference tissue. Eur. J. Nucl. Med. Mol. Imaging 2019;46:396–406.

20. Rossano S, Toyonaga T, Finnema SJ, et al. Assessment of a white matter reference region for 11C-UCB-J PET quantification. J. Cereb. Blood Flow Metab. 2019;40(9):1890–1901.

21. Mertens N, Maguire RP, Serdons K, et al. Validation of Parametric Methods for [11C]UCB-J PET Imaging Using Subcortical White Matter as Reference Tissue. Mol. Imaging Biol. 2020;22:444–452.

22. Kim SE, Choi CW, Yoon BW, et al. Crossed-Cerebellar Diaschisis in Cerebral Infarction: Technetium-99m-HMPAO SPECT and MRI. J. Nucl. Med. 1997;38:14–19.

23. Takasawa M, Watanabe M, Yamamoto S, et al. Prognostic value of subacute crossed cerebellar diaschisis: Single-photon emission CT study in patients with middle cerebral artery territory infarct. Am. J. Neuroradiol. 2002;23(2):189–193.

24. Sobesky J, Thiel A, Ghaemi M, et al. Crossed cerebellar diaschisis in acute human stroke: a PET study of serial changes and response to supratentorial reperfusion. J. Cereb. Blood Flow Metab. 2005;25:1685–1691.

25. Funck T, Al-Kuwaiti M, Lepage C, et al. Assessing neuronal density in peri-infarct cortex with PET: Effects of cortical topology and partial volume correction. Hum. Brain Mapp. 2017;38(1):326–338.

26. Miura H, Nagata K, Hirata Y, et al. Evolution of Crossed Cerebellar Diaschisis in Middle Cerebral Artery Infarction. J. Neuroimaging 1994;4(2):91–96.

27. Joya A, Padro D, Gómez-Vallejo V, et al. PET Imaging of Crossed Cerebellar Diaschisis after Long-Term Cerebral Ischemia in Rats. Contrast Media Mol. Imaging 2018;2018

28. Kushner M, Alavi A, Reivich M, et al. Contralateral cerebellar hypometabolism following cerebral insult: A positron emission tomographic study. Ann. Neurol. 1984;15(5):425–434.

29. Cramer SC, Nelles G, Benson RR, et al. A functional MRI study of subjects recovered from hemiparetic stroke. Stroke 1997;28(12):2518–2527.

30. Cao Y, D'Olhaberriague L, Vikingstad EM, et al. Pilot study of functional MRI to assess cerebral activation of motor function after poststroke hemiparesis. Stroke 1998;29(1):112–122.

31. Cramer SC, Moore CI, Finklestein SP, Rosen BR. A pilot study of somatotopic mapping after cortical infarct. Stroke 2000;31(3):668–671.

32. Tuncel H, Boellaard R, Coomans EM, et al. Kinetics and 28-day test–retest repeatability and reproducibility of [11C]UCB-J PET brain imaging. J. Cereb. Blood Flow Metab. 2021;41(6):1338–1350.

33. Stout KA, Dunn AR, Hoffman C, Miller GW. The Synaptic Vesicle Glycoprotein 2: Structure, Function, and Disease Relevance. ACS Chem. Neurosci. 2019;10(9):3927–3938.

34. Rizzoli SO, Betz WJ. Synaptic vesicle pools. Nat. Rev. Neurosci. 2005;6:57–59.

35. Denker A, Rizzoli SO. Synaptic vesicle pools: An update. Front. Synaptic Neurosci. 2010;2(OCT):135.

36. Virmani T, Kavalali ET. Synaptic vesicle recycling as a substrate for neural plasticity. Synaptic Plast. Transsynaptic Signal. 2005;255–272.

37. Warraich Z, Kleim JA. Neural plasticity: The biological substrate for neurorehabilitation. PM R 2010;2:s208–s219.

38. Emsell L, Laroy M, Van Cauwenberge M, et al. The Leuven late life depression (L3D) study: PET-MRI biomarkers of pathological brain ageing in late-life depression: study protocol. BMC Psychiatry 2021;21(1):64.

39. Cai Z, Li S, Zhang W, et al. Synthesis and Preclinical Evaluation of an 18F-Labeled Synaptic Vesicle Glycoprotein 2A PET Imaging Probe: [18F]SynVesT-2. ACS Chem. Neurosci. 2020;11(4):592–603.

40. Zheng C, Holden D, Zheng MQ, et al. A metabolically stable PET tracer for imaging synaptic vesicle protein 2A: synthesis and preclinical characterization of [18F]SDM-16. Eur. J. Nucl. Med. Mol. Imaging 2022;49(5):1482–1496.

FIGURE LEGENDS

FIGURE 1: Example delineation of lesion (red), peri-ischemic area (yellow) and unaffected ipsilesional (blue) and contralesional (green) grey matter. Images are shown in radiological convention. VOI = volume-of-interest.

FIGURE 2: Representative baseline and 6 months follow up images of 3 patients with ischemic stroke, shown in radiological convention. **A:** 85-year-old female patient with an ischemic stroke in the right MCA territory. **B:** 68-year-old female patient with a subcortical stroke in the left internal capsule. **C:** 84-year-old male patient with an ischemic stroke in the deep right MCA territory.
Our study demonstrated a further decline of synaptic density in the ischemic lesion over time, which can be appreciated in panel A (dashed white arrows). Although there was a trend towards global decrease of synaptic density over time in the unaffected ipsilesional grey matter (solid white arrows in panel A), this decrease was only significant in the ipsilesional supplementary motor area (solid white arrow in panel B). We also demonstrated crossed cerebellar diaschisis to persist over time (solid white arrows in panel C). The lesions are indicated on the baseline T2 FLAIR images with red arrow heads.
MCA = middle cerebral artery; SUVR = standardized uptake value ratio.

FIGURE 3: Localization of the ischemic lesions (n=13) at baseline in MNI (Montreal Neurological Institute) space. Lesion masks of patients with a left-sided stroke (n=4) were flipped over the mid-sagittal plane to visualize all the ipsilesional hemispheres on the right side. Color scale indicates amount of patients with involvement of the ischemic lesion at a certain location. Images are shown in radiological convention.

FIGURE 4: Individual scores on FMUE of patients at baseline and at 6 months follow up. FMUE = Fugl-Meyer upper extremity (maximum score = 66); FU = follow up.

FIGURE 5: Boxplot of cerebellar AI of 40 controls and of 13 stroke patients at baseline and follow up. A positive AI (exceeding the mean + 2 standard deviation boundaries of AI of controls) is the hallmark of crossed cerebellar diaschisis. AI = asymmetry index.

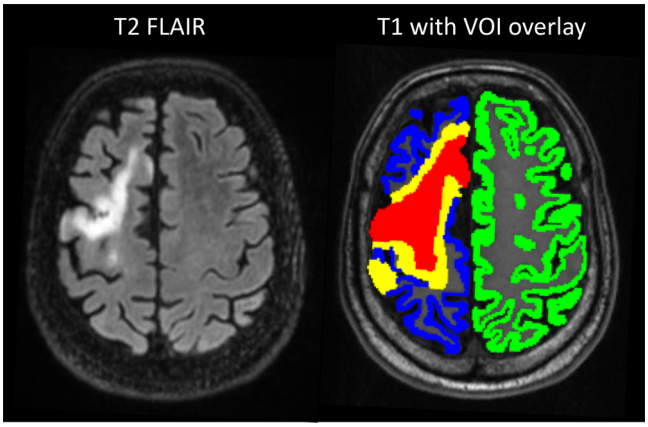

ANA_26593_Figure1.tif

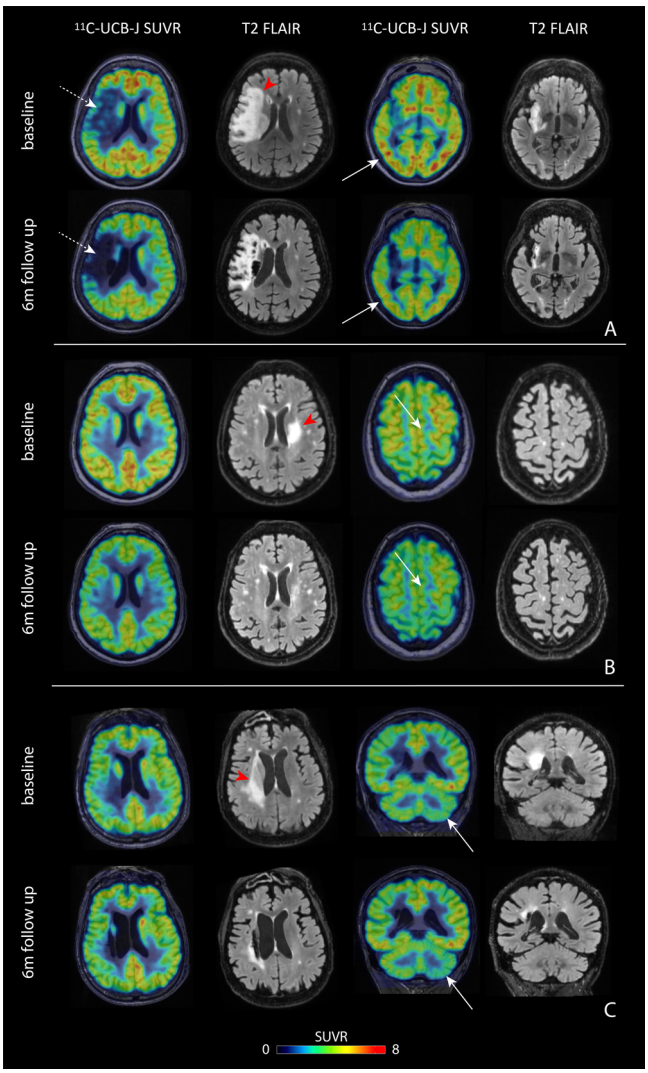

ANA_26593_Figure2.tif

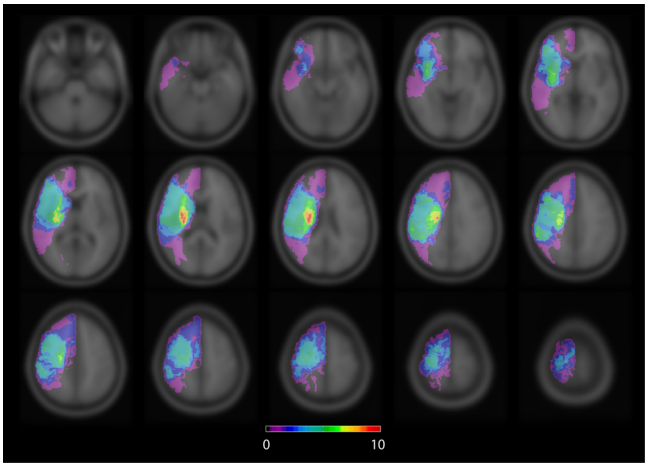

ANA_26593_Figure3.tif

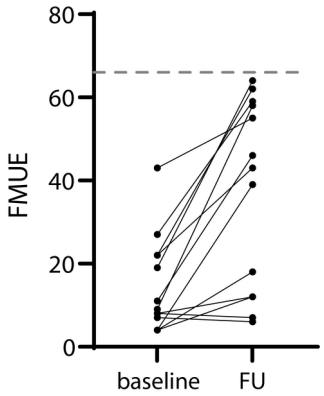

ANA_26593_Figure4.tif

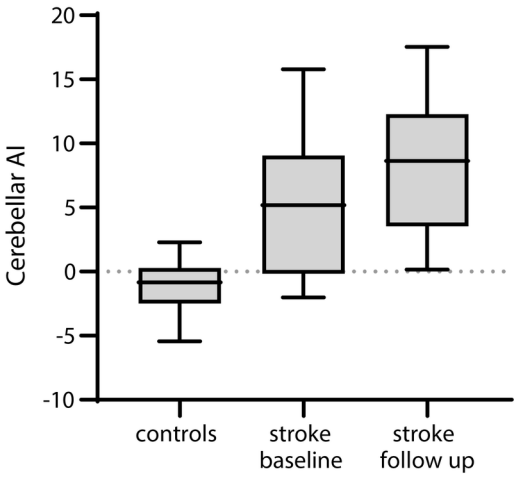

ANA_26593_Figure5.tif

TABLE 1: Demographic, clinical and neuroimaging characteristics

	Patients with ischemic stroke n = 13	
	baseline	**follow up**
Age (years, mean±SD)	67±15	
Sex (n, male/female)	5/8	
Interval between stroke and PET scan (days; mean±SD)	22±8	185±15
NIHSS (mean±SD)	10±4	/
FMUE (median [IQR])	9 [7-22]	43 [12-58]
FMLE (median [IQR])	12 [8-23]	25 [21-32]
ARAT (median [IQR])	/	30 [3-57]
FAC (median [IQR])	0 [0-1]	5 [1-5]
BI (median [IQR])	6 [3-7]	17 [10-20]
Lesion volume (ml, median [IQR])	25 [7.6-92]	24 [7.9-71]
Etiology – TOAST classification, n [%]		
large artery atherosclerosis	1 (8%)	
cardioembolism	3 (23%)	
small vessel occlusion	1 (8%)	
other determined etiology	4 (31%)	
undetermined etiology	4 (31%)	

ARAT = Action Research Arm Test; BI = Barthel Index; FAC = Functional Ambulation Categories; FMLE = Fugl-Meyer Lower Extremity; FMUE = Fugl-Meyer Upper Extremity; NIHSS = National Institutes of Health Stroke Scale; PET = positron emission tomography.

TABLE 2: Longitudinal results of ^{11}C-UCB-J SUVR (with partial volume correction) in ischemic stroke patients in brain regions potentially modifying upper limb motor recovery (without excluding lesioned voxels)

	^{11}C-UCB-J SUVR					
	ipsilesional			**contralesional**		
Volume-of-interest	baseline	follow up	*p-value*	baseline	follow up	*p-value*
primary sensorimotor cortex	6.84 (6.61-7.54)	5.70±2.52	0.19	7.62±0.95	7.21±0.92	0.18
supplementary motor area	6.96±1.79	5.61±2.67	**0.02**	7.84±0.99	7.45 (7.37-7.71)	0.19
premotor cortex	6.54±1.89	5.40±2.98	**0.0498**	7.88±0.89	7.45±0.94	0.15
prefrontal cortex	7.19±1.37	6.32±2.09	**0.04**	8.02±0.93	7.52±0.88	0.08
cingulate cortex	7.20±1.31	6.76±1.53	0.23	8.21 (6.82-8.50)	7.20±1.13	0.09
parietal cortex	7.67±1.33	6.95±1.70	0.13	8.49±1.14	8.07 (7.58-8.25)	0.13
insula	5.78±1.45	4.58±2.53	0.06	6.93 (6.68-7.68)	6.42±0.78	0.17
striatum	4.92±1.06	4.21±1.66	0.05	6.59±0.76	6.26±0.77	0.16
cerebellum	4.30±0.61	4.11±0.50	0.19	4.08±0.62	3.77±0.49	**0.049**

Significant p-values are shown in bold. SUVR = standardized uptake value ratio.

TABLE 3: Longitudinal results of ^{11}C-UCB-J SUVR (with partial volume correction) in ischemic stroke patients in brain regions potentially modifying upper limb motor recovery after excluding lesioned voxels

	^{11}C-UCB-J SUVR ipsilesional		
Volume-of-interest	baseline	follow up	*p-value*
primary sensorimotor cortex	7.57±0.84	6.76±1.28	0.07
supplementary motor area	7.54±1.23	6.72±1.43	**0.046**
premotor cortex	7.48±0.83	7.12 (5.56-7.35)	0.07
prefrontal cortex	7.69±1.00	7.15±1.02	0.06
cingulate cortex	7.37±1.24	7.00±1.24	0.20
parietal cortex	8.03±1.27	7.53 (7.03-7.80)	0.34
insula	6.44±1.32	5.54 (5.30-6.21)	0.13
striatum	6.12±1.16	5.82±0.72	0.41

Significant p-values are shown in bold. SUVR = standardized uptake value ratio.